JOURNAL OF Materials CHEMISTRY

Deposition of yttria-stabilized zirconia thin films by atomic layer epitaxy from β-diketonate and organometallic precursors

Matti Putkonen,[a] Timo Sajavaara,[b] Jaakko Niinistö,[a] Leena-Sisko Johansson[c] and Lauri Niinistö*[a]

[a]Laboratory of Inorganic and Analytical Chemistry, Helsinki University of Technology, PO Box 6100, FIN-02015 Espoo, Finland. E-mail: Lauri.Niinisto@hut.fi
[b]Accelerator Laboratory, University of Helsinki, PO Box 43, FIN-00014 Helsinki, Finland
[c]Center of Chemical Analysis, Helsinki University of Technology, PO Box 6100, FIN-02150 Espoo, Finland

Received 4th September 2001, Accepted 3rd December 2001
First published as an Advance Article on the web 23rd January 2002

Yttria-stabilised zirconia (YSZ) films were deposited by atomic layer epitaxy (ALE) using $Zr(thd)_4$, $Cp_2Zr(CH_3)_2$ and Cp_2ZrCl_2 as zirconium precursors. $Y(thd)_3$ and ozone were used as yttrium and oxygen sources, respectively. YSZ films were grown at 375 °C from $Y(thd)_3/O_3$–$Zr(thd)_4/O_3$. Deposition temperatures were 310–365 °C for the $Y(thd)_3/O_3$–$Cp_2Zr(CH_3)_2/O_3$ and 275–350 °C for the $Y(thd)_3/O_3$–Cp_2ZrCl_2/O_3 precursor combinations. Growth rates with a Y to Zr pulsing ratio of 1 : 1 were 0.56, 0.79 and 0.89 Å $(cycle)^{-1}$ when $Zr(thd)_4$, $Cp_2Zr(CH_3)_2$ and Cp_2ZrCl_2 were used as zirconium precursors, respectively. Crystallinity and surface morphology of the deposited films were characterised by XRD and AFM while TOF-ERDA, XRF and SEM-EDX were used to analyse stoichiometry and possible impurities. The YSZ films were (100) oriented when deposited with a Y to Zr pulsing ratio of 1 : 1. Only thinner films (<60 nm), deposited from $Y(thd)_3/O_3$–$Zr(thd)_4/O_3$, showed the (111) preferred orientation. The lattice parameter was in the range of 5.09–5.28 Å when the Y_2O_3 content was 5–89 mol%. When Cp_2ZrCl_2 was used as zirconium precursor, 0.1–1.7 mol% chlorine was observed in the films. According to the AFM analysis, roughness was dependent on the pulsing ratio of the Y and Zr precursors.

1. Introduction

Due to its thermal and chemical stability yttria-stabilized zirconia (YSZ) is an attractive material for optical and electrical applications. ZrO_2 has three different structural polymorphs, of which the monoclinic phase is thermodynamically stable at room temperature. Volume changes attributed to polymorphic phase transformations restrict high temperature applications of ZrO_2 thin films. The cubic form of ZrO_2 thin films is usually stabilised by adding other oxides, typically Y_2O_3, but Sc_2O_3,[1] CaO,[2] CeO_2,[3–5] In_2O_3,[6] Gd_2O_3,[7] MgO,[2,7] Al_2O_3[1,8] and $MgAlO_3$[9] have also been used.

YSZ has been used as a buffer layer for high-T_c superconducting,[10–12] ferroelectric[13–15] and pyroelectric[16] films as well as for protective coatings on $YBa_2Cu_3O_{7-\delta}$.[17] It has also been studied for field effect transistor (FET) type oxygen sensors.[18] Due to its comparatively high relative permittivity ($\varepsilon = 10-31$),[10,19,20] YSZ is among the candidates for gate oxide in memory applications such as dynamic random access memories (DRAMs),[21,22] although YSZ does not provide a relative permittivity high enough for >1 Gb DRAMs.[23,24] Other interesting applications of YSZ include thermal barrier coatings where thick YSZ film (~100–500 µm) has been used as such or with bond coatings, for example (Ni,Co)CrAlY.[25,26] Due to their high ionic conductivity, thicker YSZ films have also been studied as solid electrolytes in oxygen pumps,[27] solid-oxide fuel cells[28] and oxygen membranes.[29]

Both physical and chemical gas phase techniques as well as sol–gel[30,31] processes have been applied for the deposition of YSZ thin films. Physical vapor deposition methods such as electron beam evaporation,[15,32] sputtering[33–35] and pulsed laser deposition[36–38] have been frequently used. Chemical vapor deposition (CVD) methods include spray pyrolysis,[39–41] electrochemical vapor deposition[42] as well as conventional,[43] aerosol[44] and plasma assisted CVD.[45–47] In the CVD processes, volatile zirconium precursors employed are typically the β-diketonates, such as $Zr(thd)_4$[48–50] and $Zr(acac)_4$,[51] (thd = 2,2,6,6-tetramethylheptane-3,5-dionate and acac = acetylacetonate) but also $ZrCl_4$,[52,53] alkoxides[54,55] and compounds with tetradentate Schiff-base ligands[56] have been used. The selection of yttrium precursors has been more limited; only the use of $Y(thd)_3$[43,51] or YCl_3[52,53] has been reported. YSZ depositions by CVD have been reported for a wide temperature range depending on the precursors used and the reactor set-up. CVD depositions using halides precursors have been carried out above 1100 °C[53,52] while YSZ depositions have been reported at 450–850 °C with β-diketonates as precursors, although reproducible results have been obtained only at 600 °C and above.[48] Lower deposition temperatures (400–600 °C) have been achieved only in plasma-activated CVD processes.[46]

Atomic layer epitaxy (ALE),[57] also referred to as atomic layer deposition (ALD) or atomic layer CVD (ALCVD), has been successfully used for the deposition of several oxide films.[58–60] The self-limiting growth mechanism of ALE relies on alternate saturative reactions on the substrate surface. This makes the deposition process especially suitable for those applications where exact film thickness is needed or where the depositions are performed onto uneven or porous substrates.[61–63]

Recently, ALE has also been applied for the deposition of Y_2O_3 and ZrO_2 thin films. Yttrium oxide thin films have been deposited from β-diketonate precursors and ozone,[64,65] while ZrO_2 has been prepared from $ZrCl_4$ and H_2O at 300–500 °C[66–68] Furthermore, ZrO_2 films have been deposited by ALE using $Zr(thd)_4$, Cp_2ZrCl_2 or $Cp_2Zr(CH_3)_2$ as precursors, together with O_3.[69] In this paper we report the results of yttria-stabilized zirconia depositions by atomic layer epitaxy

 DOI: 10.1039/b107799f

This journal is © The Royal Society of Chemistry 2002

using $Zr(thd)_4$, $Cp_2Zr(CH_3)_2$ and Cp_2ZrCl_2 as zirconium precursors. $Y(thd)_3$ was used as the yttrium source and ozone as oxidising agent.

2. Experimental

Cp_2ZrCl_2 (Strem Chemicals, #93-4002, 99%) (Cp = cyclopentadiene, C_5H_5), $Cp_2Zr(CH_3)_2$ and $Zr(thd)_4$ were used as zirconium precursors. $Cp_2Zr(CH_3)_2$ and $Zr(thd)_4$ were prepared according to published methods by Samuel and Rausch,[70] and Morozova *et al.*,[71] respectively. $Y(thd)_3$ was synthesised according to Eisentraut and Sievers.[72] Precursor properties and their applicability to ALE depositions of binary oxides have previously been examined.[65,69]

Films were deposited in a commercial flow-type hot-wall Atomic Layer Epitaxy (ALE) reactor F-120 manufactured by ASM Microchemistry Ltd. Film depositions were carried out at 2–3 mbar pressure onto Si(100) and soda lime glass substrates measuring 10 × 5 cm^2. O_3 was used as oxidiser and it was generated from O_2 (99.999%) in an ozone generator (Fischer model 502). Nitrogen (>99.999%, Schmidlin UHPN 3000 N_2 generator) was used as carrier and purging gas.

Film thicknesses were evaluated using the optical fitting method as described by Ylilammi and Ranta-aho.[73] Reflectance and transmittance spectra were measured in a Hitachi U-2000 double beam spectrophotometer. Crystallinity and crystallite orientations of the deposited films were determined by X-ray diffraction using Cu Kα radiation (Philips MPD 1880). Surface morphology was studied by Nanoscope III atomic force microscope (Digital Instruments) operating in tapping mode. Samples were measured with a scanning frequency of 1–2 Hz. Several wide scans (10–20 μm) were performed from different parts of samples to check the uniformity of the sample. Final images were measured with a scanning area of 2 × 2 μm. Roughness values were calculated as root mean square values (rms).

The yttrium to zirconium ratio as well as the amount of chlorine impurities were measured by X-ray fluorescence in a Philips PW 1480 WDS spectrometer using Rh excitation. Data were analysed with the Uniquant 4.34 program (Omega Data Systems, Netherlands), which is based on fundamental parameters and experimentally determined instrumental sensitivity factors.[74] A scanning electron microscope (Zeiss DSM 962) with an energy-dispersive X-ray spectrometer (Link Isis 100) (SEM/EDX) was used to verify the Y to Zr ratio obtained by the XRF method. Measurements were carried out with 4, 5 and 8 kV acceleration voltage keeping the beam current at 1 nA. SiO_2 was used as Si and O standard and $(Y,Zr)O_2$ (14.37% Y) as Y and Zr standard. The Strata-program was used to calculate the film composition and final thickness.

TOF-ERDA measurements were carried out at the Accelerator Laboratory of the University of Helsinki. In this method[75] heavy ions are projected into the sample and the signal consists of forward recoiling sample atoms ejected by the ion beam. Both velocity and energy for recoiled atoms are determined using timing gates and a charged particle detector, which enables differentiation of masses. In the case of YSZ, signals originating from adjacent masses of yttrium and zirconium can not be separated. Therefore, only some selected samples were analysed in order to study the oxygen content and impurity levels of deposited YSZ films and not the yttrium to zirconium ratio. With known stopping power and scattering cross sections, elemental depth distributions can also be calculated. For these TOF-ERDA studies, a 53 MeV $^{127}I^{10+}$ ion beam was used, obtained from a 5 MV tandem accelerator EGP-10-II. Samples were measured at 20° tilt and the recoils were detected at 40° with respect to the incoming beam. For heavy recoil, energy spectra were obtained from the TOF signals and hydrogen spectra from the charged particle detector.

Surface composition and YSZ film chemistry were also investigated using X-ray photoelectron spectroscopy (XPS). The measurements were carried out with an AXIS 165 spectrometer (Kratos Analytical) at the HUT Center for Chemical Analysis using monochromated Al Kα irradiation at 100 W. Air-exposed samples were measured as received and from the surface only. The area of analysis was 1 mm^2. For surface composition, wide scans were recorded using an 80 eV analyser pass energy and 1 eV step. For more detailed chemical information, high-resolution spectra of the C 1s, Y 3d, Zr 3d and O 1s regions were recorded using a 20 eV analyser pass energy and 0.1 eV step. Using similar high-resolution acquisition parameters and experimental set-up, the FWHM of Ag 3d 5/2 line in clean silver specimen was recorded to be 0.55 eV. During the data acquisition the insulating sample surfaces were neutralised with slow thermal electrons.[76] For the identification of the chemical compounds, the binding energies were charge-corrected using the C–C component of the C 1s signal at 285 eV as an internal standard.[77]

3. Results and discussion

3.1 ALE growth of YSZ films

The temperature regions where the deposition is surface-controlled, *i.e.* the ALE window,[78] were observed in earlier studies for the binary Y_2O_3[65] and ZrO_2[69] oxides. Different precursor combinations and the optimal deposition temperatures are listed in Table 1 together with growth rates of the binary Y_2O_3 and ZrO_2. Since Y_2O_3 can be deposited in quite a wide temperature range, the deposition range for surface-controlled YSZ growth therefore mainly depends on the selection of the zirconium precursor. YSZ films were prepared by incorporating $Y(thd)_3/O_3$ cycles with different ZrO_2 processes (Fig. 1). When $Zr(thd)_4$ was used as the zirconium

Table 1 ALE deposition temperatures and the measured deposition rates of Y_2O_3 and ZrO_2 thin films from different precursors[65,69]

Process	ALE window/°C	Growth rate/Å $(cycle)^{-1}$
$Y(thd)_3/O_3$	250–375	0.23
$Zr(thd)_4/O_3$	375–400	0.24
Cp_2ZrCl_2/O_3	310–365	0.53
$Cp_2Zr(CH_3)_2/O_3$	275–350	0.55

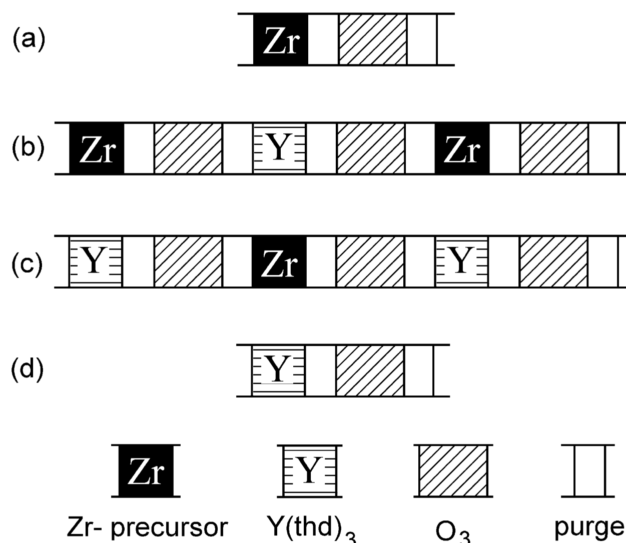

Fig. 1 Pulsing sequences used in the deposition of ZrO_2 (a) and Y_2O_3 (d) as well as YSZ with pulsing ratios of 1 : 2 (b) and 2 : 1 (c).

precursor, films were deposited at 375 °C. Wider temperature regions of 310–365 °C and 275–350 °C were studied when the $Cp_2Zr(CH_3)_2$ and Cp_2ZrCl_2 precursors were used for the deposition of zirconium oxide, respectively. At first, YSZ films were deposited from different precursors using a Y to Zr precursor pulsing ratio of 1 : 2 and by changing the deposition temperature. Sufficiently long reactant pulse times were employed to obtain surface saturation on the substrate. Regardless of the deposition temperature, growth rate and crystallinity of the deposited films were quite constant. Therefore, more detailed studies of the thin film depositions were carried out only at one selected temperature, namely at 350 and 300 °C when $Cp_2Zr(CH_3)_2$ and Cp_2ZrCl_2 were used as zirconium precursors, respectively.

The deposition rate was investigated more closely by depositing YSZ thin films and changing the yttrium to zirconium precursor pulsing ratio. Measured growth rate was compared to the values calculated using the growth rates of binary oxides. Regardless of the Zr precursor, an increase in growth rate was observed with an increasing Y to Zr pulsing ratio (Fig. 2). Indeed, the maximum growth rate was 10–23% higher, depending on the precursors and pulsing ratio used. It is interesting to note that although in the $Y(thd)_3/O_3$–Cp_2ZrCl_2/O_3 process a 23% increase in growth rate was obtained, the increase in the similar process using $Cp_2Zr(CH_3)_2$ was only 10%, reflecting different behaviour of the organometallic precursors. In our earlier study,[69] the growth rate of ZrO_2 from $Cp_2Zr(CH_3)_2/O_3$ was approximately 4% larger compared to the Cp_2ZrCl_2/O_3 process. A possible explanation for the different behaviour of organometallic zirconium precursors lies in the differences of surface chemistries during the deposition process. As actual growth rates of separate oxides can not be measured from the deposited mixed oxides, it remains unclear whether the Y_2O_3 or ZrO_2 growth rate has increased. Recently, a similar quite pronounced effect in the ALE growth rate of $SrTiO_3$ thin film was reported,[79] where a 2.6 times higher growth rate as a function of pulsing ratio was observed.

Growth rates with a fixed Y to Zr precursor pulsing ratio of 1 : 1 were 0.56, 0.79 and 0.89 Å $(cycle)^{-1}$ when $Zr(thd)_4$, $Cp_2Zr(CH_3)_2$ and Cp_2ZrCl_2 were used as zirconium precursors, respectively. To verify the surface-controlled growth mechanism, YSZ films were deposited with different reactant pulse times. Growth rates were constant when pulse times of 1–3 s were used for $Y(thd)_3$ and zirconium precursors together with 1.5–4 s pulse durations for O_3, indicating an ALE-type deposition mechanism. After optimising deposition parameters, the thickness of the YSZ films could be simply determined by the number of deposition cycles (Fig. 3) as should be the case in an ideally behaving ALE process.[78] Refractive indices of the films were 2.17–2.14 regardless of the selected zirconium

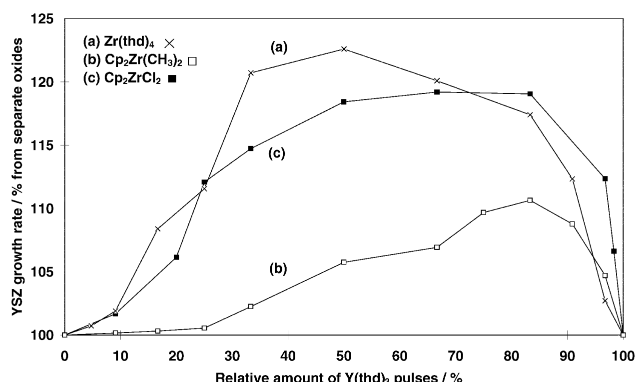

Fig. 2 YSZ film growth rate compared with the separate Y_2O_3 and ZrO_2 film growth rates. Pulsing ratio is expressed as a relative amount of $Y(thd)_3$ pulses, calculated from the number of metal precursor pulses in one cycle by the formula: 100 × $Y(thd)_3/(Y(thd)_3$ + Zr precursor pulses).

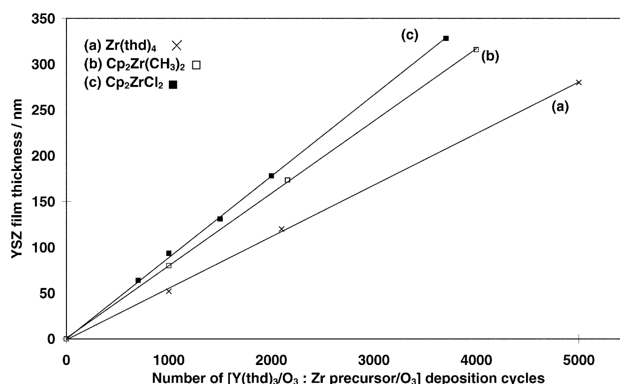

Fig. 3 Thickness of YSZ films as a function of number of deposition cycles when a 1 : 1 pulsing ratio was used.

precursor and pulsing ratio, which corresponds well to the previously reported values.[80,81] However, the refractive index of the yttrium-rich films decreased down to 1.90 with an increasing yttrium content. YSZ film adhesion was tested by the tape test.[82] No peeling was observed regardless of the substrate, precursor pulsing ratio or deposition temperature.

3.2 YSZ film analysis

Although yttrium content in films was not linearly dependent on the pulsing ratio, it was easily controllable by the number of $Y(thd)_3/O_3$ pulses (Fig. 4). It also depended on the Zr precursor used as according to XRF and SEM/EDX measurements, YSZ films containing 31.4, 16.3 and 15.8 mol% Y_2O_3 were obtained with a constant Y to Zr precursor pulsing ratio of 1 : 1 when $Zr(thd)_4$, $Cp_2Zr(CH_3)_2$ and Cp_2ZrCl_2 were used as zirconium precursors, respectively. According to TOF-ERDA, impurity levels were generally low (Table 2). Films deposited by the 1 : 1 pulsing ratio at 375 °C from $Y(thd)_3/O_3$–$Zr(thd)_4/O_3$ contained 1.7 at% of hydrogen and 0.4 at% of carbon, while films with the

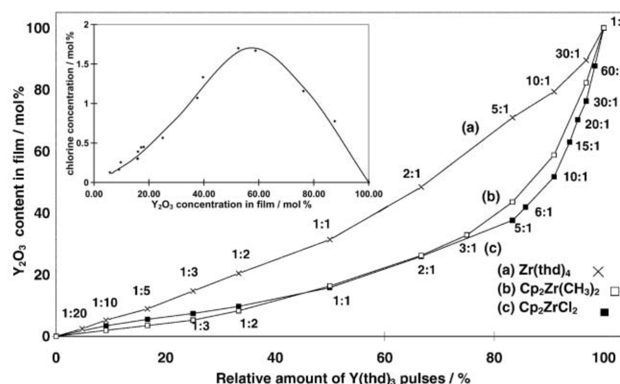

Fig. 4 Y_2O_3 content in the deposited films as the function of pulsing ratio of $Y(thd)_3/O_3$–$Zr(thd)_4/O_3$ (a), $Y(thd)_3/O_3$–$Cp_2Zr(CH_3)_2/O_3$ (b) and $Y(thd)_3/O_3$–Cp_2ZrCl_2/O_3 (c). Zirconium precursor pulsing times of 1.0 s and O_3 pulsing time of 2.0 s were used and the deposition temperatures were 375 (a), 350 (b) and 300 °C (c). Pulsing ratios 0% and 100% represent pure ZrO_2 and Y_2O_3 films, respectively. Inset shows the chlorine content in films deposited from $Y(thd)_3/O_3$–Cp_2ZrCl_2/O_3 as a function of the Y_2O_3 concentration.

Table 2 TOF-ERDA results of impurity levels of the YSZ thin films deposited from different precursor combinations onto Si(100) substrates

Precursors		Pulsing ratio	Carbon/ at%	Hydrogen/ at%	Fluorine/ at%
$Y(thd)_3$	$Zr(thd)_4$	1 : 1	0.4	1.7	0.5
$Y(thd)_3$	$Cp_2Zr(CH_3)_2$	1 : 1	<0.1	0.13	0.4
$Y(thd)_3$	Cp_2ZrCl_2	1 : 1	1.1	0.5–1.0	0.3

lowest impurity levels (around 0.1 at%) were obtained by using the $Y(thd)_3/O_3$–$Cp_2Zr(CH_3)_2/O_3$ precursor combination. Also notable amounts of fluorine (0.3–0.5 at%) were detected in the films which probably originated from the Teflon gaskets or perfluorinated vacuum greases of the reactor.

The stoichiometry of the films was calculated using metal to oxygen ratios obtained from TOF-ERDA data and yttrium to zirconium ratios obtained from XRF measurements. In the previous study, both Y_2O_3 and ZrO_2 thin films had a slight oxygen excess regardless of the precursor used.[69] In the case of stoichiometric YSZ films, oxygen content should depend on the yttrium oxide content raising the metal to oxygen ratio above 0.50 (pure ZrO_2), with an increasing Y_2O_3 content. A 1 : 1 pulsing ratio of $Y(thd)_3/O_3$–$Zr(thd)_4/O_3$ precursors resulted in films with a slight oxygen excess (metal to oxygen ratio of 0.54). A stoichiometric metal to oxygen ratio would be 0.57 at this yttrium content (31.4 mol%). It is interesting to note that when organometallic zirconium precursors were used, oxygen contents in films were close to stoichiometric *i.e.* the oxygen to metal ratio was 0.53 and 0.55 when a 1 : 1 pulsing ratio in the $Y(thd)_3/O_3$–$Cp_2Zr(CH_3)_2/O_3$ and $Y(thd)_3/O_3$–Cp_2ZrCl_2/O_3 processes was used, respectively. Stoichiometric metal to oxygen ratio value at this yttrium content (around 16 mol%) is 0.54.

In our previous study, ZrO_2 thin films deposited from Cp_2ZrCl_2/O_3 resulted in chlorine-free films when depositions were carried out above 275 °C.[69] However, Cl contamination of YSZ films was observed regardless of the deposition temperature or pulsing ratio. According to XRF, the chlorine content was in the range of 1.5–0.25 mol% when films were deposited with the 2 : 1 pulsing ratio at 275–350 °C, respectively. Furthermore, in films deposited with 1 : 5–5 : 1 pulsing ratios of $Y(thd)_3/O_3$–Cp_2ZrCl_2/O_3 at 300 °C, the chlorine content increased from 0.1 to 1.7 mol%. (Fig. 4, inset). Chlorine contamination was also observed by TOF-ERDA. It is interesting to note that some films deposited with the $Y(thd)_3/O_3$–$Zr(thd)_4/O_3$ process contained chlorine (0.2 at% according to TOF-ERDA). This probably originated from the precursor synthesis procedure,[71] in which $ZrCl_4$ was used as a reagent.

Crystallite orientations in the films deposited onto Si(100) and soda lime glass substrates were analysed by XRD as a function of the deposition temperature, film thickness and pulsing ratio. Films were identified to have a polycrystalline cubic structure. According to our earlier study,[69] crystallinity of the ZrO_2 films, deposited using Cp_2ZrCl_2/O_3 as precursors, was greatly enhanced when the deposition temperature was increased from 275 °C to 350 °C. However, an increase in the deposition temperature seems to have no effect on the crystallinity of the YSZ films deposited inside the ALE window. In addition, orientations of YSZ films deposited with the Y to Zr precursor pulsing ratio of 1 : 1 from different precursors were analysed as a function of film thickness. Thin films ($<$60 nm) were (111) oriented when deposited from $Y(thd)_3/O_3$–$Zr(thd)_4/O_3$. However, when the thickness of these films increased the (200) reflection became most intense, but weak (111), (220) and (311) reflections were observed as well (Fig. 5a,d). YSZ films deposited from zirconium cyclopentadiene precursors were (100) oriented regardless of the film thickness. Minor intensity (111), (220) and (311) reflections were also present as in the β-diketonate case. Both the crystallinity and orientation of the deposited films were dependent on the pulsing ratio of the precursors regardless of the substrate used. Maximum film crystallinity was observed when 1 : 1–2 : 1 pulsing ratios of $Y(thd)_3/O_3$–$Cp_2Zr(CH_3)_2/O_3$ or $Y(thd)_3/O_3$–Cp_2ZrCl_2/O_3 processes were employed. $Zr(thd)_4$ as a precursor produced maximum film crystallinity with the 1 : 5–1 : 2 pulsing ratio. With all Zr precursors, predominantly (100) oriented films were obtained with the Y to Zr 1 : 1 pulsing ratio. When other pulsing ratios were used, relative intensities of the (111), (220) and (311) reflections increased. Peak widths (FWHM) measured from the (200) reflection for the YSZ films were 0.20–0.32° 2θ depending on the precursors and pulsing ratio chosen (Fig. 6). Regardless of the zirconium precursor used, YSZ reflections became slightly broader with an increasing Y_2O_3 content while a minimum in peak widths was observed in the same region where the films were most crystalline.

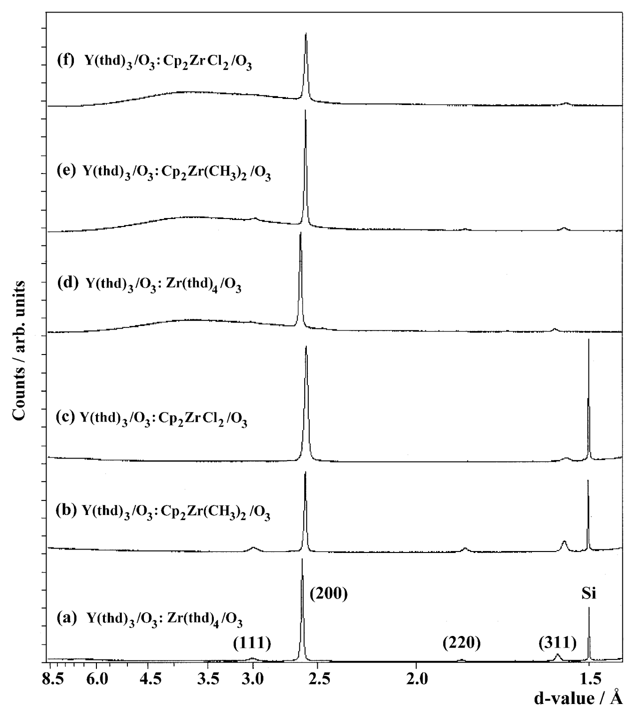

Fig. 5 XRD patterns of YSZ film deposited by different precursors onto Si(100) (a–c) and soda lime glass (d–f) by the 1 : 1 pulsing ratio. Deposition temperatures were 375 (a,d), 350 (b,e) and 300 °C (c,f). Thicknesses of films were in the range of 170–200 nm. Diffraction peaks identified according to JCPDS card 30–1468.

The lattice parameter of the YSZ films was calculated from the diffraction patterns using the *d*-spacing of the (200) reflection. A cubic phase was observed when Y_2O_3 content was above 5 mol%. The lattice parameter was 5.09–5.28 Å when Y_2O_3 content was 5–89 mol% depending on the pulsing ratio of the precursors (Table 3). Values obtained at this region were in good agreement with the previously reported values for thin films[46,48] and bulk YSZ[83] (Fig. 6). It should be noted that according to the phase diagram of bulk YSZ,[84] the cubic phase is supposed to exist in a narrower Y_2O_3 concentration region. However, cubic YSZ thin films have previously been prepared

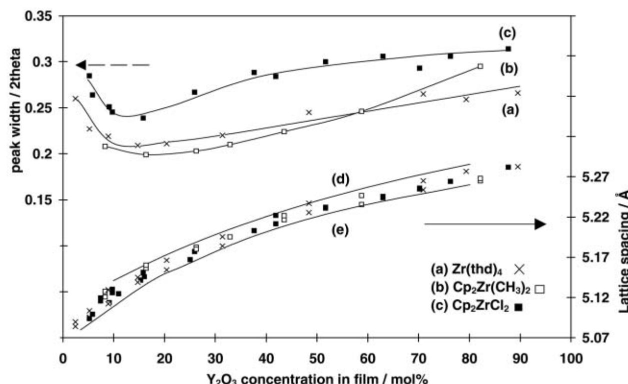

Fig. 6 Lattice parameter of cubic YSZ as a function of the Y_2O_3 concentration in the films (bottom). Solid lines (d) and (e) represent previously published values of YSZ lattice parameters in the bulk[83] and thin films,[46] respectively. Dependence of the (200) peak width on the Y_2O_3 content is also presented (a–c).

Table 3 Yttrium oxide content and lattice parameter of deposited films as a function of precursor pulsing ratio for different precursor combinations. O_3 was used as an oxidiser

Precursors		Pulsing ratio	Mol% Y_2O_3	Lattice spacing/Å
$Y(thd)_3$	$Zr(thd)_4$	1 : 10 – 30 : 1	5.2–89	5.10–5.28
$Y(thd)_3$	$Cp_2Zr(CH_3)_2$	1 : 2 – 30 : 1	8.3–82	5.12–5.26
$Y(thd)_3$	Cp_2ZrCl_2	1 : 5 – 60 : 1	5.5–88	5.09–5.28

by several methods in a wide range of Y_2O_3 content. For example, cubic YSZ thin films with 5–10 mol% of Y_2O_3 have been prepared by CVD at 750 °C and above.[48] Furthermore, cubic YSZ films with 3.5–80 mol% Y_2O_3 have been obtained by plasma-assisted CVD at 500 °C.[46]

YSZ film surface morphology was analysed by AFM (Fig. 7). A series of YSZ films were deposited with different $Y(thd)_3/O_3$–Zr precursor/O_3 pulsing ratios. Depositions were carried out at 375, 350 and 300 °C with $Zr(thd)_4$, $Cp_2Zr(CH_3)_2$ and Cp_2ZrCl_2 as zirconium precursors, respectively. Typically the film roughness in ALE deposited binary oxide films has been dependent on the film thickness as was the case for instance in Y_2O_3[65] and ZrO_2.[69] Therefore, it was attempted to keep the thickness of the deposited films constant, *i.e.* in the range of 100–150 nm. A series of YSZ films were deposited with a different Y_2O_3 concentration. Fig. 8 represents AFM images of YSZ films with 8–9 mol% Y_2O_3. Regardless of the precursor used, films were uniform and roughness was slightly dependent on the process used. Furthermore, film roughness appeared to be only dependent on the pulsing ratio of precursors (Fig. 8). Films deposited from $Y(thd)_3/O_3$–$Zr(thd)_4/O_3$ were slightly rougher compared to the films deposited using organometallic zirconium precursors.

For the XPS studies two binary and three YSZ oxide films were chosen, all deposited at 300 °C. YSZ films were deposited with pulsing ratios of 1 : 2, 1 : 1 and 5 : 1 using $Y(thd)_3/O_3$–Cp_2ZrCl_2/O_3 precursor combination. According to the XRF measurements the Y_2O_3 contents of the films were 9.7 mol%, 15.8 mol% and 37.6 mol% depending on the pulsing ratios given above, respectively. The freshly prepared but air-exposed films were measured as received, without sputter cleaning, since even mild ion bombardment may easily distort oxide chemistry. Instead, the adventitious carbon contamination layer, which is typical of air exposed surfaces, was used as internal binding energy standard. We have also found that the carbonaceous contamination layer has often acted as a nonreacting passivation layer at the oxide–vacuum interface.[85] Each sample was

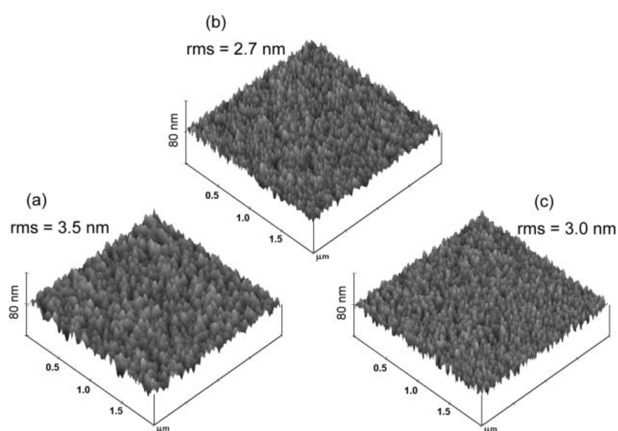

Fig. 7 AFM images of YSZ films deposited onto Si(100) substrate (a) from $Y(thd)_3/O_3$–$Zr(thd)_4/O_3$ at 375 °C, (b) from $Y(thd)_3/O_3$–$Cp_2Zr(CH_3)_2/O_3$ at 350 °C and (c) from $Y(thd)_3/O_3$–Cp_2ZrCl_2/O_3 at 300 °C. Film thicknesses were in the range of 110–140 nm. Depth scale: 20 nm from black to white.

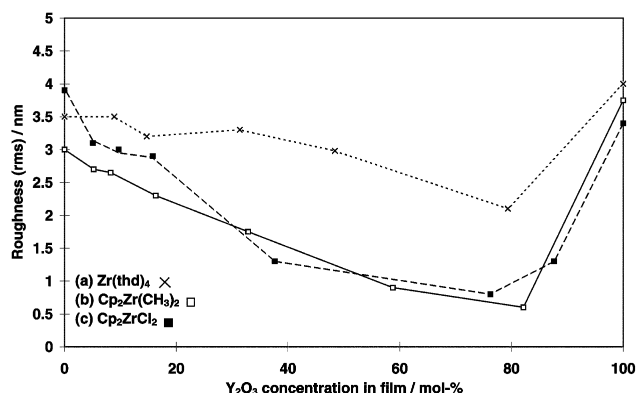

Fig. 8 Roughness of YSZ films as a function of precursor pulsing ratio measured by AFM. Film thickness was 100–150 nm. Roughness values of binary Y_2O_3 and ZrO_2 oxide films with a thickness of 130 nm were taken from refs 65 and 69, respectively.

measured at 2–3 different locations. No major differences between the measuring points were observed indicating uniformity of films. Apart from Y, Zr and O, only carbon and small amounts of fluorine were detected in XPS wide scans. The spectra indicated that fluorine was present as surface contamination only, since the F 1s electron signal was not followed by inelastic background tailing the peak.[86] The carbon detected came mainly from the surface contamination layer.

The high-resolution spectra of Y 3d, Zr 3d O 1s and C 1s (for binding energy reference) regions were also recorded. For the pure binary oxides, the binding energies of yttrium, zirconium and oxygen were in good accordance with the tabulated values.[87] Y 3d was recorded at 156.7 eV and Zr 3d at 182.2 eV as sharp, well resolved doublets. In the case of oxygen, the main component of O 1s was at 529.8 eV for the Y_2O_3 and 530.0 eV for the ZrO_2, while the minor component at 531.8 eV in both cases could be ascribed to surface –OH groups and water molecules adsorbed on the oxide surface. However, the high-resolution results for the YSZ films turned out to be quite interesting. The binding energies of both Zr 3d, Y 3d and that assigned to the oxide component of O 1s were clearly dependent on the Zr to Y ratio of the film, while the peaks linked to –OH groups and surface carbon did not shift, see Fig. 9. For the sample with 37.6 mol% of Y_2O_3 a shift as large as 0.5 eV was observed. Our observations differ somewhat from those reported on YSZ single crystal studies by

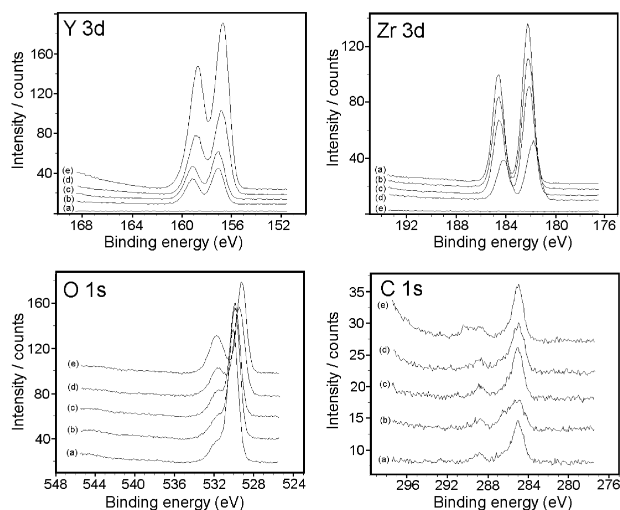

Fig. 9 XPS high resolution spectra of the of Y 3d, Zr 3d, O 1s, and C 1s regions of YSZ film deposited onto Si(100) at 300 °C using $Y(thd)_3/O_3$–Cp_2ZrCl_2/O_3 precursor combination with a pulsing ratios of (a) 0 : 1 (ZrO_2), (b) 1 : 2, (c) 1 : 1, (d) 5 : 1 and (e) 1 : 0 (Y_2O_3).

Parmigiani *et al.*[88] However, in that study only samples with Y_2O_3 contents of 12–24 mol% were investigated. The XPS results are in good agreement with XRD data indicating lattice modifications introduced by the increasing Y_2O_3 content.

4. Conclusions

Surface-controlled ALE deposition of crystalline YSZ was achieved at 275–375 °C depending on the precursor system selected. These temperatures are significantly lower than reported earlier in the literature for thin film depositions of YSZ by the CVD methods. Constant growth rates of 0.56 Å $(cycle)^{-1}$ for $Y(thd)_3/O_3$–$Zr(thd)_4/O_3$, 0.79 Å $(cycle)^{-1}$ for $Y(thd)_3/O_3$–$Cp_2Zr(CH_3)_2/O_3$ and 0.89 Å $(cycle)^{-1}$ $Y(thd)_3/O_3$–Cp_2ZrCl_2/O_3 were obtained when the Y to Zr precursor pulsing ratio of 1 : 1 was used. The films were crystalline regardless of the deposition temperature and precursor used. Films were polycrystalline cubic YSZ with preferred (100) orientation. Only thinner films (< 60 nm) deposited by $Y(thd)_3/O_3$–$Zr(thd)_4/O_3$ were (111) oriented. The pulsing ratio of the precursors affected the crystallinity and orientation of the films. Films deposited by the 1 : 1 pulsing ratio were (100) oriented regardless of the precursor used whereas the intensity of the (222), (211) and (311) reflections increased if other pulsing ratios were used. The lattice parameter was 5.09–5.28 Å when the Y_2O_3 content was 5–89 mol% Y_2O_3, produced by different precursor pulsing ratios. YSZ films deposited by the optimised parameters contained less than 1 at% of hydrogen and carbon when $Cp_2Zr(CH_3)_2$ or Cp_2ZrCl_2 were used as zirconium precursors.

Acknowledgement

The authors wish to thank Professor P. Hautojärvi, Laboratory of Physics, for providing facilities for the AFM measurements. Also, we are grateful to Mr Jyrki Juhanoja, Lic. Phil., for performing the SEM/EDX analysis.

References

1 S. B. Quadri, E. F. Skelton, M. Harford, P. Lubitz and L. Aprigliano, *J. Vac. Sci. Technol., A*, 1990, **8**, 2344.
2 F. Hanus and L. D. Laude, *Appl Surf. Sci.*, 1998, **127–129**, 544.
3 R. Di Maggio, A. Tomasi and P. Scardi, *Mater. Lett.*, 1997, **31**, 345.
4 A. Galtayries, M. Crucifix, G. Blanchard, G. Terwagne and R. Sporken, *Appl. Surf. Sci.*, 1999, **142**, 159.
5 A. N. Khodan, J.-P. Contour, D. Michel, O. Durand, R. Lyonnet and M. Mihet, *J. Cryst. Growth*, 2000, **209**, 828.
6 S. B. Qadri, H. R. Khan, E. F. Skelton and P. Lubitz, *Surf. Coat. Technol.*, 1998, **100–101**, 94.
7 F. Tcheliebou, M. Boulouz and A. Boyer, *J. Mater. Res.*, 1997, **12**, 3260.
8 A. Nazeri and S. B. Qadri, *Surf. Coat. Technol.*, 1996, **86–87**, 166.
9 Y. Takahashi, T. Kawae and M. Nasu, *J. Cryst. Growth*, 1986, **74**, 409.
10 J. Qiao and C. Y. Yang, *Mater. Sci. Eng.*, 1995, **R14**, 157.
11 Y. J. Tian, S. Linzen, F. Schmidl, A. Matthes, H. Schneidewind and P. Seidel, *Thin Solid Films*, 1999, **338**, 224.
12 W. Prusseit, S. Corsépius, M. Zwerger, P. Berberich, H. Kinder, O. Eibl, C. Jaekel, U. Breuer and H. Kurz, *Physica C*, 1992, **201**, 249.
13 H. N. Lee, S. Senz, N. D. Zakharov, C. Harnagea, A. Pignolet, D. Hesse and U. Gösele, *Appl. Phys. Lett.*, 2000, **77**, 3260.
14 Z. Trajanovic, C. Kwon, M. C. Robson, K.-C. Kim, M. Rajeswari, R. Ramesh, T. Venkatesan, S. E. Lofland, S. M. Bhagat and D. Fork, *Appl. Phys. Lett.*, 1996, **69**, 1005.
15 K. Tokita and H. Hoshi, *Jpn. J. Appl. Phys.*, 2000, **39**, 5399.
16 Y. Q. Xu, A. Ignatiev and N. J. Wu, *Proc. IEEE Int. Symp. Appl. Ferroelectr., 6th*, 1998, 199.
17 R. Aguiar, F. Sánchez, C. Ferrater and M. Varela, *Thin Solid Films*, 1997, **306**, 74.
18 Y. Miyahara, K. Tsukuda and H. Miyagi, *J. Appl. Phys.*, 1988, **63**, 2431.
19 T. Hirai, K. Teramoto, K. Nagashima, H. Koike, S. Matsuno, S. Tanimoto and Y. Tarui, *Jpn. J. Appl. Phys.*, 1996, **35**, 4016.
20 Y. Miyahara, *J. Appl. Phys.*, 1992, **71**, 2309.
21 R. M. Wallace and G. D. Wilk, *Semicond. Int.*, 2001, **24**(8), 227.
22 A. I. Kingon, J.-P. Maria and S. K. Streiffer, *Nature*, 2000, **406**, 1032.
23 P. Singer, *Semicond. Int.*, 1992, **15**(10), 32.
24 R. Singh and R. K. Ulrich, *Interface*, 1999, **8**(2), 26.
25 M. J. Stiger, N. M. Yanar, M. G. Topping, F. S. Pettit and G. H. Meier, *Z. Metallkd.*, 1999, **90**, 1069.
26 K. Yasuda, S. Suenaga, H. Inagaki, Y. Goto, H. Takeda and K. Wada, *J. Mater. Sci.*, 2000, **35**, 317.
27 G. Garcia, A. Figueras, J. Casado, J. Llibre, M. Mokchah, G. Petot-Ervas and J. Calderer, *Thin Solid Films*, 1998, **317**, 241.
28 K.-W. Chour, J. Chen and R. Xu, *Thin Solid Films*, 1997, **304**, 106.
29 J. Han, G. Xomeritakis and Y. S. Lin, *Solid State Ionics*, 1997, **93**, 263.
30 S.-Y. Bae, C.-S. Kim and Y.-J. Oh, *J. Appl. Phys.*, 1999, **85**, 5226.
31 P. Peshev and V. Slavova, *Mater. Res. Bull.*, 1992, **27**, 1269.
32 M. Hartmanová, I. Thurzo, M. Jergel, J. Bartoš, F. Kadlec, V. Zelezný, D. Tunega, F. Kundracik, S. Chromik and M. Brunel, *J. Mater. Sci.*, 1988, **33**, 969.
33 M. Nagashima, S.-i. Nakano, K. Sasaki and T. Hata, *Jpn. J. Appl. Phys.*, 1999, **38**, L74.
34 T. Hata, K. Sasaki, Y. Ichikawa and K. Sasaki, *Vacuum*, 2000, **59**, 381.
35 V. V. Naumov, V. F. Bochkarev, O. S. Trushin and A. A. Goryachev, *Neorg. Mat.*, 1998, **34**, 57; *Inorg. Mater.*, 1998, **34**, 46.
36 P. Tiwari, S. Sharan and J. Narayan, *J. Appl. Phys.*, 1991, **69**, 8358.
37 D. K. Fork, D. B. Fenner, G. A. N. Connell, J. M. Phillips and T. H. Geballe, *Appl. Phys. Lett.*, 1990, **57**, 1137.
38 J. C. Delgado, F. Sánchez, R. Aquiar, Y. Maniette, C. Ferrater and M. Varela, *Appl. Phys. Lett.*, 1996, **68**, 1048.
39 Y. Matsuzaki, M. Hishinuma and I. Yasuda, *Thin Solid Films*, 1999, **340**, 72.
40 E. M. Kelder, O. C. J. Nijs and J. Schoonman, *Solid State Ionics*, 1994, **68**, 5.
41 P. Bohac and L. Gauckler, *Solid State Ionics*, 1999, **119**, 317.
42 H. Sasaki, C. Yakawa, S. Otoshi, M. Suzuki and M. Ippommatsu, *J. Appl. Phys.*, 1993, **74**, 4608.
43 G. Garcia, J. Casado, J. Llibre and A. Figueras, *J. Cryst. Growth.*, 1995, **156**, 426.
44 H. B. Wang, C. R. Xia, G. Y. Meng and D. K. Peng, *Mater. Lett.*, 2000, **44**, 23.
45 K.-i. Itoh and O. Matsumoto, *Thin Solid Films*, 1999, **345**, 29.
46 H. Holzschuh and H. Suhr, *Appl. Phys. Lett.*, 1991, **59**, 470.
47 C.-B. Cao, J.-T. Wang, W.-J. Yu, D.-K. Peng and G.-Y. Meng, *Thin Solid Films*, 1994, **249**, 163.
48 S.-C. Hwang, H.-G. Lee and H.-S. Shin, *Korean J. Chem. Eng.*, 1998, **15**, 243.
49 C. Dubordieu, S. B. Kang, Y. Q. Li, G. Kulesha and B. Gallois, *Thin Solid Films*, 1999, **339**, 165.
50 G. Garcia, A. Figueras, R. I. Merino, V. M. Orera and J. Llibre, *Thin Solid Films*, 2000, **370**, 173.
51 J. S. Kim, H. A. Marzouk and P. J. Reucroft, *Thin Solid Films*, 1995, **254**, 33.
52 M. F. Carolan and J. N. Michaels, *Solid State Ionics*, 1987, **25**, 207.
53 H. Yamane and T. Hirai, *J. Cryst. Growth*, 1989, **94**, 880.
54 K. L. Merkle, G.-R. Bai, Z. Li, C.-Y. Song and L. J. Thompson, *Phys. Status Solidi A*, 1998, **166**, 73.
55 T. Matsuzaki, N. Okuda, K. Shinozaki, N. Mizutani and H. Funakubo, *Jpn. J. Appl. Phys.*, 1998, **37**, 6229.
56 J. A. Belot, R. J. McNeely, A. Wang, C. J. Reedy, T. J. Marks, G. P. A. Yap and A. L. Rheingold, *J. Mater. Res.*, 1999, **14**, 12.
57 T. Suntola, A. Pakkala and S. Lindfors, US Patent 4413022, 1983.
58 L. Niinistö, M. Ritala and M. Leskelä, *Mater. Sci. Eng. B*, 1996, **41**, 23.
59 L. Niinistö, *Curr. Opin. Solid State Mater. Sci.*, 1998, **3**, 147.
60 L. Niinistö, *Proceedings of the International Semiconductor Conference*, 23rd edn., IEEE, Piscataway, NJ, 2000, p. 33.
61 K. Kukli, J. Ihanus, M. Ritala and M. Leskelä, *J. Electrochem. Soc.*, 1997, **144**, 300.
62 M. Utriainen, S. Lehto, L. Niinistö, Cs. Dücsõ, N. Q. Khanh, Z. E. Horváth, I. Bársony and B. Pécz, *Thin Solid Films*, 1997, **297**, 39.
63 M. Ritala, M. Leskelä, J.-P. Dekker, C. Mutsaers, P. J. Soininen and J. Skarp, *Chem. Vap. Deposition*, 1999, **5**, 7.

64 H. Mölsä, L. Niinistö and M. Utriainen, *Adv. Mater. Opt. Electron.*, 1994, **4**, 389.
65 M. Putkonen, T. Sajavaara, L.-S. Johansson and L. Niinistö, *Chem Vap. Deposition*, 2001, **7**, 44.
66 M. Ritala and M. Leskelä, *Appl. Surf. Sci.*, 1994, **75**, 333.
67 M. Copel, M. Gribelyuk and E. Gusev, *Appl. Phys. Lett.*, 2000, **76**, 436.
68 E. P. Gusev, M. Copel, E. Cartier, D. Buchanan, H. Okorn-Schmidt, M. Gribelyuk, D. Falcon, R. Murphy, S. Molis, I. J. R. Baumvol, C. Krug, M. Jussila, M. Tuominen and S. Haukka, *Proc. Electrochem. Soc.*, 2000, **2**, 477.
69 M. Putkonen and L. Niinistö, *J. Mater. Chem.*, 2001, **11**, 3141.
70 E. Samuel and M. D. Rausch, *J. Am. Chem. Soc.*, 1973, **95**, 6263.
71 N. B. Morozova, I. K. Igumenov, V. N. Mit'kin, K. V. Kradenov, O. G. Potapova, V. B. Lazarev and Ya. Kh. Grinberg, *Zh. Neorg. Khim.*, 1989, **34**, 1193; *Russ. J. Inorg. Chem.*, 1989, **24**, 672.
72 K. J. Eisentraut and R. E. Sievers, *J. Am. Chem. Soc.*, 1965, **87**, 5254.
73 M. Ylilammi and T. Ranta-aho, *Thin Solid Films*, 1993, **232**, 56.
74 UniQuant Version 2 User Manual, Omega Data Systems, Veldhoven, Netherlands, 1994.
75 J. Jokinen, J. Keinonen, P. Tikkanen, A. Kuronen, T. Ahlgren and K. Nordlund, *Nucl. Instrum. Methods Phys. Res., Sect. B*, 1996, **119**, 533.
76 Axis 165 Operating Manual and User's Guide, Kratos Analytical Ltd, Manchester, 1995.
77 G. Beamson and D. Briggs, *High resolution XPS of Organic Polymers*, Wiley, Chichester 1992.
78 T. Suntola, *Handbook of Thin Film Process Technology*; ed. D. A. Glocker and S. I. Shah, Institute of Physics, Bristol, 1995, pp. B1.5 1–17.
79 M. Vehkamäki, T. Hatanpää, T. Hänninen, M. Ritala and M. Leskelä, *Electrochem. Solid-State Lett.*, 1999, **2**, 504.
80 E. Vasco, L. Vázquez, M. Aguiló and C. Zaldo, *J. Cryst. Growth*, 2000, **209**, 883.
81 D. L. Wood, K. Nassau and T. Y. Kometani, *Appl. Opt.*, 1990, **29**, 2485.
82 B. N. Chapman, *J. Vac. Sci. Technol.*, 1974, **11**, 106.
83 R. P. Ingel and D. Lewis III, *J. Am. Ceram. Soc.*, 1986, **69**, 325.
84 V. S. Stubican, R. C. Hink and S. P. Ray, *J. Am. Ceram. Soc.*, 1978, **61**, 17.
85 H. Heikkinen, L.-S. Johansson, E. Nykänen and L. Niinistö, *Appl. Surf. Sci.*, 1998, **133**, 205.
86 S. Tougaard, *J. Electron Spectrosc. Relat. Phenom.*, 1990, **52**, 243.
87 *Handbook of X-ray photoelectron spectroscopy*, eds J. Chastain and R. C. King Jr., Physical Electronics, Eden Prairie, 1995.
88 F. Parmigiani, L. E. Depero, L. Sangaletti and G. Samoggia, *J. Electron Spectrosc. Relat. Phenom.*, 1993, **63**, 1.